

SPINOR-HELICITY CALCULATION OF THE $g^*g^* \rightarrow q\bar{q}V^*$
AMPLITUDE AT THE TREE LEVEL*

JAN FERDYAN

Institute of Theoretical Physics, Jagiellonian University
Łojasiewicza 11, 30-348 Kraków, Poland
`jan.ferdyan@student.uj.edu.pl`

BŁAŻEJ RUBA

Department of Mathematical Sciences, University of Copenhagen
Universitetsparken 5, 2100 Copenhagen, Denmark
`btr@math.ku.dk`

*Received 4 June 2024, accepted 4 September 2024,
published online 20 September 2024*

We compute amplitudes for the $g^*g^* \rightarrow q\bar{q}V^*$ process (two virtual gluons into a quark, an antiquark, and a boson) at the tree level using the spinor-helicity formalism. The resulting analytic expressions are much shorter than squared amplitudes obtained using trace methods. Our results can be used to expedite numerical calculations in phenomenological studies of the Drell–Yan process in high-energy factorization framework.

DOI:10.5506/APhysPolB.55.9-A2

1. Introduction

The Drell–Yan process [1] is a good probe for an internal structure of hadrons in proton–proton or proton–antiproton collisions. In this process, a pair of lepton and antilepton is produced by an electroweak boson — a virtual photon γ^* or Z^0 . The measured dilepton distributions can be used to determine the Drell–Yan structure functions, see *e.g.* [1]. On the other hand, the structure functions can be predicted within QCD description based on factorization schemes: collinear or high-energy factorization (also referred to as k_T factorization) [2–5]. The necessary input to these descriptions are parton distribution functions (PDFs), which parameterize the details of the proton structure. For the collinear factorization, one applies collinear parton distribution functions, which are functions of the parton energy and

* Funded by SCOAP³ under Creative Commons License, CC-BY 4.0.

of the factorization scale. In the case of high-energy factorization, one uses transverse momentum distributions (TMDs) [6], which depend also on the parton transverse momentum k_T .

Recent measurements of the Drell–Yan process in the Z^0 -mass peak region at the LHC [7] exhibit a deviation from theoretical predictions of perturbative QCD [8–12] at next-to-next-to leading order (NNLO) in the Lam–Tung combination [13] of the structure functions. One of the proposed explanations is that the Lam–Tung relation breaking may occur as a result of the parton transverse momenta [14, 15].

In the high-energy factorization, the TMDs are probed for $x \ll 1$, where x is the fraction of the hadron longitudinal momentum carried by the parton. In this kinematical regime, the proton structure is strongly dominated by the gluons. Following [15, 16], we adopt the approximation in which the quark and antiquark components of the proton structure are neglected. We consider the contribution to the Drell–Yan process which occurs by scattering of two virtual gluons g^*g^* into a quark, an antiquark, and an electroweak boson V^* that decays into a dilepton l^+l^- . The Drell–Yan structure functions depend on the gluon TMDs, so we can use measured data to constrain them. This requires however an efficient evaluation of the matrix elements of the $g^*g^* \rightarrow q\bar{q}V^*$ process that speeds up the fitting procedure.

We remark that the Drell–Yan process occurs also through the channel $q_{\text{val}}g^* \rightarrow qV^*$ [15, 17, 18], involving a valence quark q_{val} , which we do not consider in this paper. It is important when the density of valence quarks q_{val} is high. This is the case for $x \sim 0.1$ in the forward–backward region, in which the V boson is produced almost collinearly with the incoming parton. We are most interested in central production, in which $x \ll 1$, so the contribution of valence quarks is small (they have a low parton density).

Direct evaluation of the relevant Feynman diagrams used in [15] leads to very long and numerically costly expressions. In order to improve the efficiency, we apply the spinor-helicity formalism. The use of spinors in the study of scattering amplitudes is by now standard, see *e.g.* [19, 20]. We use notation for spinors which is a small adaptation of the one commonly used in general relativity [21].

Similar scattering processes were considered in [22], where authors studied also the possibility of multi-gluon production and performed numerical calculations. The amplitudes were calculated in terms of pure spinor contractions, based on the techniques from [19]. However, explicit formulas for the amplitudes directly in terms of momenta of the scattering particles were not provided. Such expressions, presented in a compact analytic form, are the main result of our work. We also present example calculations, illustrating the methods we used to obtain our results.

The $g^*g^* \rightarrow q\bar{q}V^*$ process was also studied in [15, 16, 23], where the amplitudes squared were calculated numerically applying the standard trace approach within the k_T -factorization framework. Such amplitudes can be also derived within the Color Glass Condensate (CGC) framework [17, 18] by considering the low gluon density limit.

1.1. Kinematics

We consider production of a virtual electroweak boson in a high-energy proton–proton collision. We are interested in the process illustrated in figure 1. The protons momenta P_1 and P_2 are near light-like, and in the center-of-mass system can be expressed in Minkowskian coordinates as

$$P_1 \approx \left(\sqrt{S}/2, 0, 0, \sqrt{S}/2 \right), \quad P_2 \approx \left(\sqrt{S}/2, 0, 0, -\sqrt{S}/2 \right). \quad (1.1)$$

The collision invariant energy squared is $S = (P_1 + P_2)^2$. We work in the k_T -factorization framework, so partons carry nonzero transverse momenta. The full momentum k_i of the gluon originating from the i^{th} proton can be decomposed as

$$k_i = x_i P_i + k_{iT}, \quad i = 1, 2. \quad (1.2)$$

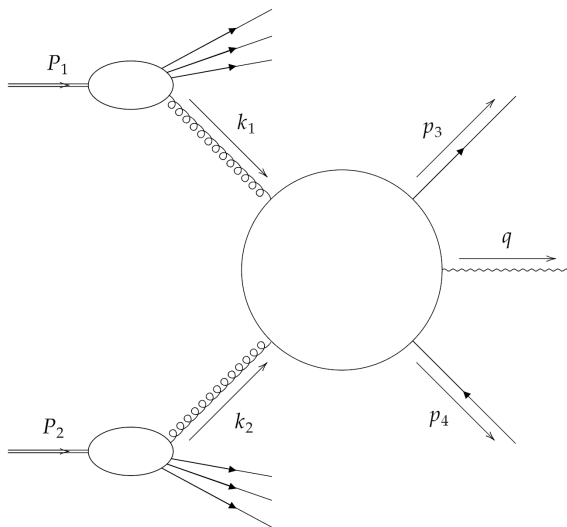


Fig. 1. General form of the diagrams. Big circle represents all possible QCD LO subdiagrams. P_1, P_2 are the momenta of the incoming protons, k_1, k_2 are momenta of virtual gluons emitted by the corresponding protons, p_3, p_4 are the momenta of the quark and antiquark, and q is the momentum of the emitted electroweak boson.

Here, x_i is the fraction of P_i carried by the gluon and k_{iT} is the momentum in the plane perpendicular to the scattering plane ($k_{iT} \cdot P_1 = k_{iT} \cdot P_2 = 0$). The gluon polarizations are approximated as¹ $\epsilon^\mu(k_i) = x_i P_i^\mu / \sqrt{-k_{iT}^2}$ [2–5, 16].

We denote the momentum of the boson V^* as q and the momenta of outgoing quark and antiquark as p_3 and p_4 , respectively.

1.2. The method and results

We use the spinor-helicity formalism to obtain simple analytic formulas for the Feynman diagrams describing the $g^* g^* \rightarrow q \bar{q} V^*$ process at the tree level.

The correctness of our calculations has been checked by comparing numerically with amplitudes squared, summed over polarizations of q and \bar{q} , obtained using standard trace methods. The numerical treatment was necessary because analytic formulas for traces obtained using the algebra of γ matrices are so lengthy that it does not seem feasible to analyze them using symbolic algebra software (let alone pen and paper).

The manuscript is organized as follows. Section 2 explains our conventions for two component spinors and bispinors. In particular, in Subsections 2.3 and 2.4, we construct polarization spinors satisfying massless or massive Dirac equation. These choices of spinor bases do not affect physical observables, such as cross sections, but they do affect the amplitudes². In Subsection 2.5, we provide explicit expressions in terms of components for various spinorial objects, *e.g.* the dictionary between spinor components and space-time components of a vector. The main results are shown in Section 3. We present the Feynman diagrams and the corresponding algebraic expressions, and then decompose the amplitudes according to colors and chiralities. In Subsection 3.2, we evaluate the resulting expressions using spinors in the massless case. These amplitudes are less general than our final result, but due to the significant simplifications, we deemed them worthy of displaying separately. In Subsection 3.3, we give formulas for amplitudes allowing for nonzero masses of the quark and antiquark. Even though the amplitudes are significantly more complicated than in the massless case, they are still multiple orders of magnitude shorter than outputs of calculations done with using trace methods. In Subsection 3.4, we present example calculations of amplitudes for some specific diagrams. We comment on possible directions for further research in Section 4.

¹ More precisely, one uses also a Ward identity: the amplitude is orthogonal to k_i^μ , thus contraction with k_{iT} can be replaced by contraction with $-x_i P_i$.

² Simply put, amplitudes are tensors in the space of polarizations and one has to specify in which basis are their components given.

2. Spinor-helicity formalism

2.1. Spinor indices and bases

We denote (two component) spinor indices with uppercase Latin indices, with an overdot used for indices in the complex conjugate representation. Invariant tensors $\varepsilon_{AB}, \varepsilon_{\dot{A}\dot{B}}$ (related to each other by complex conjugation) are used for raising and lowering of indices

$$\varepsilon_{AB}\varepsilon^{CB} = \delta_A^C, \quad (2.1a)$$

$$\xi_B = \xi^A \varepsilon_{AB}, \quad (2.1b)$$

$$\xi^A = \varepsilon^{AB} \xi_B, \quad (2.1c)$$

and analogously for conjugate spinor indices. The order of indices in the above formulas matters because $\varepsilon_{AB}, \varepsilon_{\dot{A}\dot{B}}$ are skew-symmetric. Thus, for example,

$$\xi^A \eta_A = -\xi_A \eta^A. \quad (2.2)$$

A pair $A\dot{A}$ of spinor indices may be traded for one Lorentz index. This is achieved by contracting with $(\sigma^\mu)_{A\dot{A}}, (\bar{\sigma}^\mu)^{\dot{A}A}$, which are vectors of spinorial matrices

$$v_{A\dot{A}} = v_\mu (\sigma^\mu)_{A\dot{A}}, \quad v^{\dot{A}A} = v_\mu (\bar{\sigma}^\mu)^{\dot{A}A}, \quad (2.3)$$

where $\bar{\sigma}$ is related to σ by raising of spinor indices combined with matrix transposition. Given two Lorentz vectors, we can contract them directly or contract their spinor indices. The results differ by a factor of 2

$$u_{A\dot{A}} v^{\dot{A}A} = 2u_\mu v^\mu. \quad (2.4)$$

Another important property of σ and $\bar{\sigma}$ is that their product, symmetrized in Lorentz indices, gives Minkowski metric

$$\sigma^\mu \bar{\sigma}^\nu + \sigma^\nu \bar{\sigma}^\mu = 2g^{\mu\nu} \mathbb{1} \quad \implies \quad v_{A\dot{A}} v^{\dot{A}B} = v_\mu v^\mu \delta_A^B. \quad (2.5)$$

With the aid of the inner product, we can readily obtain the general representation of a spinor in terms of components. We choose any pair of spinors o and ι normalized as

$$o_A \iota^A = 1. \quad (2.6)$$

Then $\{o, \iota\}$ form a basis of the spinor space. The decomposition of a general spinor ξ in this basis reads

$$\xi = \xi^0 o + \xi^1 \iota, \quad \text{where} \quad \xi^0 = \xi_A \iota^A, \quad \xi^1 = -\xi_A o^A, \quad (2.7)$$

and the invariant tensors decompose as

$$\varepsilon_{AB} = o_A \iota_B - \iota_A o_B, \quad \varepsilon_{\dot{A}\dot{B}} = \bar{o}_{\dot{A}} \bar{\iota}_{\dot{B}} - \bar{\iota}_{\dot{A}} \bar{o}_{\dot{B}}. \quad (2.8)$$

Now, we define a null tetrad of world-vectors as

$$\begin{aligned} l_+^{\dot{A}A} = o^A \bar{o}^{\dot{A}} &\iff l_+^\mu = \frac{1}{2} o^A \sigma_{A\dot{A}}^\mu \bar{o}^{\dot{A}}, \\ l_-^{\dot{A}A} = \iota^A \bar{\iota}^{\dot{A}} &\iff l_-^\mu = \frac{1}{2} \iota^A \sigma_{A\dot{A}}^\mu \bar{\iota}^{\dot{A}}, \\ m^{\dot{A}A} = o^A \bar{\iota}^{\dot{A}} &\iff m^\mu = \frac{1}{2} o^A \sigma_{A\dot{A}}^\mu \bar{\iota}^{\dot{A}}, \\ \bar{m}^{\dot{A}A} = \iota^A \bar{o}^{\dot{A}} &\iff \bar{m}^\mu = \frac{1}{2} \iota^A \sigma_{A\dot{A}}^\mu \bar{o}^{\dot{A}}. \end{aligned} \quad (2.9)$$

Using the above null basis, we can construct a standard orthonormal basis for Minkowski space — a Minkowski tetrad $\{t^\mu, x^\mu, y^\mu, z^\mu\}$

$$\begin{aligned} l_\pm = t \pm z &\iff t = \frac{1}{2} (l_+ + l_-), \quad z = \frac{1}{2} (l_+ - l_-), \\ m = x + iy, \quad \bar{m} = x - iy &\iff x = \frac{1}{2} (m + \bar{m}), \quad y = \frac{1}{2i} (m - \bar{m}). \end{aligned} \quad (2.10)$$

In principle, we could start with the null tetrad or Minkowski tetrad, and construct from them a spinor basis $\{o, \iota\}$, unique up to an overall sign (the same for o and ι).

2.2. Dirac bispinors

A Dirac bispinor is a pair of two spinors

$$\psi = \begin{bmatrix} \xi_A \\ \bar{\eta}^{\dot{A}} \end{bmatrix}, \quad \bar{\psi} = [\eta^A \quad \bar{\xi}_{\dot{A}}], \quad (2.11)$$

where $\bar{\psi}$ is the Dirac conjugate of ψ . It is clear from the above definition that the identity $\bar{\psi}_1 \psi_2 = \overline{\psi_2 \psi_1}$ holds. We work with a chiral representation of gamma matrices

$$\gamma^\mu = \begin{bmatrix} 0 & \sigma^\mu \\ \bar{\sigma}^\mu & 0 \end{bmatrix}, \quad \gamma_5 = \begin{bmatrix} -\mathbb{1} & 0 \\ 0 & \mathbb{1} \end{bmatrix}. \quad (2.12)$$

We will also use the eigenprojections of γ_5

$$P_\pm = \frac{1 \pm \gamma_5}{2}. \quad (2.13)$$

For any Lorentz vector n , we define the matrix

$$\hat{n} = n_\mu \gamma^\mu = \begin{bmatrix} 0 & n_\mu \sigma^\mu \\ n_\mu \bar{\sigma}^\mu & 0 \end{bmatrix} = \begin{bmatrix} 0 & n_{A\dot{A}} \\ n^{\dot{A}A} & 0 \end{bmatrix}. \quad (2.14)$$

2.3. Spinor bracket notation

We will now construct a convenient basis of bispinors satisfying the massless Dirac equation.

We choose a reference spinor $\rho^A \neq 0$ and define a future-directed null vector l by $l^{A\dot{A}} = \rho^A \bar{\rho}^{\dot{A}}$. For every null, future directed, real Lorentz vector n with $n \cdot l \neq 0$, we introduce the angle and square bra and ket spinors

$$|n] = \begin{bmatrix} \theta(n)_A \\ 0 \end{bmatrix}, \quad |n\rangle = \begin{bmatrix} 0 \\ \frac{1}{\theta(n)^{\dot{A}}} \end{bmatrix}, \quad [n| = [\theta(n)^A \quad 0], \quad \langle n| = [0 \quad \overline{\theta(n)}_{\dot{A}}], \quad (2.15)$$

where $\theta(n)_A = \frac{1}{\sqrt{2|n \cdot l|}} n_{A\dot{A}} \bar{\rho}^{\dot{A}}$. Then $|n]$, $|n\rangle$, resp. $[n|$, $\langle n|$ form bases of solutions of

$$\hat{n}\psi = 0, \quad \text{resp.} \quad \bar{\psi}\hat{n} = 0. \quad (2.16)$$

The normalization factor $\frac{1}{\sqrt{2|n \cdot l|}}$ is needed for the normalization of the current

$$\bar{\psi}\gamma^\mu\psi = 2n^\mu. \quad (2.17)$$

We remark that the factor $\frac{1}{\sqrt{2|n \cdot l|}}$ makes our solutions singular when n is colinear with l . This is just a singularity of the chosen basis and depends on the choice of the reference spinor.

The spinors defined in (2.15) are eigenvectors of γ_5

$$\gamma_5|n] = -|n], \quad \gamma_5|n\rangle = |n\rangle, \quad [n|\gamma_5 = -[n|, \quad \langle n|\gamma_5 = \langle n|, \quad (2.18)$$

thus the basis vectors defined in (2.15) correspond to particles of fixed chirality (and hence also helicity). Spinors of different helicity are orthogonal, *e.g.* we have $\langle n_1 | n_2] = 0$ and (since γ^μ flips chirality) $[n_1 | \gamma^\mu | n_2] = 0$.

2.4. Massive Dirac bispinors

For a Lorentz vector p with $p^2 = m^2 > 0$, we define the brackets as

$$\begin{aligned} |p] &= \begin{bmatrix} \theta(p)_A \\ \frac{\phi(p)}{\theta(p)^{\dot{A}}} \end{bmatrix}, & |p\rangle &= \begin{bmatrix} -\phi(p)_A \\ \theta(p)^{\dot{A}} \end{bmatrix}, \\ [p| &= [\theta(p)^A \quad -\overline{\phi(p)}_{\dot{A}}], & \langle p| &= [\phi(p)^A \quad \overline{\theta(p)}_{\dot{A}}], \end{aligned} \quad (2.19)$$

where

$$\theta(p)_A := \frac{p_{A\dot{A}} \bar{\rho}^{\dot{A}}}{\sqrt{2|p \cdot l|}}, \quad \phi(p)_A := \frac{m}{\sqrt{2|p \cdot l|}} \rho_A. \quad (2.20)$$

This reduces to the definition in (2.15) for $m \rightarrow 0$, thus the notation is consistent.

The constructed spinors satisfy the Dirac equation

$$(\hat{p} - m) |p\rangle = (\hat{p} - m) |p\rangle = 0 = [p | (\hat{p} - m) = \langle p | (\hat{p} - m) . \quad (2.21)$$

Unlike in the massless case, spinor brackets have no singularities because $p \cdot l \neq 0$ for all vectors p with $p^2 > 0$. Another difference is that the direction of their spin depends on the reference spinor. More precisely, we have eigenequations for the spinor operator $S_p = \frac{1}{2p \cdot l} \gamma_5 [\hat{p}, \hat{l}]$

$$S_p |p\rangle = -|p\rangle, \quad S_p |p\rangle = |p\rangle, \quad [p | S_p = -[p |, \quad \langle p | S_p = \langle p |. \quad (2.22)$$

We describe a particle with momentum p (a future-directed vector) with kets $|p\rangle$ or $|p]$, depending on the value of the spin. For an antiparticle, we use instead the spinors $|-p\rangle, |-p]$ (note that definitions in (2.19) and (2.20) make sense both for future and past-directed vectors).

We will now prove useful symmetries of spinor brackets, which allow to reduce the number of amplitudes that we will need to compute by a factor 2. Let us consider the charge conjugation \mathcal{C} which acts on bispinors in the following way:

$$\mathcal{C}\psi = \mathcal{C} \begin{bmatrix} \xi_A \\ \bar{\eta}^{\dot{A}} \end{bmatrix} = \begin{bmatrix} \eta_A \\ \bar{\xi}^{\dot{A}} \end{bmatrix}. \quad (2.23)$$

The operator \mathcal{C} is antilinear, $\mathcal{C}^2 = \mathbb{1}$ and it anticommutes with gamma matrices γ^μ and γ_5 . Now, we can define another operator

$$\mathcal{Q} := \gamma_5 \mathcal{C}, \quad (2.24)$$

which satisfies

$$\mathcal{Q}^2 = -\mathbb{1}, \quad \mathcal{Q}\gamma_5\mathcal{Q}^{-1} = -\gamma_5, \quad \mathcal{Q}\gamma^\mu\mathcal{Q}^{-1} = \gamma^\mu. \quad (2.25)$$

We also have, for any bispinors ψ_1, ψ_2

$$\overline{\mathcal{Q}\psi_1} \mathcal{Q}\psi_2 = \overline{\psi_1} \psi_2. \quad (2.26)$$

It can be also directly shown that for bispinor brackets, we have the following identities:

$$\mathcal{Q}|p\rangle = |p\rangle, \quad \mathcal{Q}|p\rangle = -|p\rangle. \quad (2.27)$$

With the help of the above identities, we will derive useful symmetries. Let us begin with the contraction with Γ being any composition of the gamma matrices

$$\begin{aligned} [p_3 | \Gamma | p_4\rangle &= \overline{[p_3]} \Gamma |p_4\rangle = \overline{\mathcal{Q}[p_3]} \Gamma \mathcal{Q}|p_4\rangle = \overline{\mathcal{Q}[p_3]} \mathcal{Q} \Gamma |p_4\rangle \\ &= \overline{[p_3]} \Gamma |p_4\rangle = \langle p_3 | \Gamma | p_4], \end{aligned} \quad (2.28)$$

and similarly

$$[p_3 | \Gamma | p_4] = -\overline{\mathcal{Q}[p_3]} \Gamma \mathcal{Q} | p_4 \rangle = -\overline{\mathcal{Q}[p_3]} \mathcal{Q} \Gamma | p_4 \rangle = -\overline{[p_3] \Gamma | p_4} \rangle = -\overline{\langle p_3 | \Gamma | p_4 \rangle}. \quad (2.29)$$

These symmetries hold for both the massless and massive case.

Since \mathcal{Q} anticommutes with γ_5 , it exchanges the projections $\mathcal{Q}P_{\pm}\mathcal{Q}^{-1} = P_{\mp}$. Therefore, if we now define Γ_{\pm} to be a composition of the gamma matrices and one of the projections P_{\pm} , the symmetries (2.28) and (2.29) translates to

$$[p_3 | \Gamma_{\pm} | p_4] = \overline{\mathcal{Q}[p_3]} \Gamma_{\pm} \mathcal{Q} | p_4 \rangle = \overline{\mathcal{Q}[p_3]} \mathcal{Q} \Gamma_{\mp} | p_4 \rangle = \overline{\langle p_3 | \Gamma_{\mp} | p_4 \rangle}, \quad (2.30)$$

and

$$[p_3 | \Gamma_{\pm} | p_4] = -\overline{\mathcal{Q}[p_3]} \mathcal{Q} \Gamma_{\mp} | p_4 \rangle = -\overline{\langle p_3 | \Gamma_{\mp} | p_4 \rangle}. \quad (2.31)$$

2.5. Component expressions

We will work with null tetrad defined as in Subsection 2.1. Vectors can be written with components with respect to chosen basis as

$$n^{\mu} = n^{+} l_{+}^{\mu} + n^{-} l_{-}^{\mu} + n^{\perp} m^{\mu} + n^{\bar{\perp}} \bar{m}^{\mu} = \begin{pmatrix} n^{+} & n^{-} & n^{\perp} & n^{\bar{\perp}} \end{pmatrix}^{\mu}, \quad (2.32)$$

where

$$n^{\pm} = n^0 \pm n^3, \quad n^{\perp} = n^1 + i n^2, \quad n^{\bar{\perp}} = n^1 - i n^2. \quad (2.33)$$

The correspondence with spinor components is

$$n^{\dot{A}A} = \begin{pmatrix} n^{\dot{0}0} & n^{\dot{0}1} \\ n^{\dot{1}0} & n^{\dot{1}1} \end{pmatrix} = \begin{pmatrix} n^{+} & n^{\bar{\perp}} \\ n^{\perp} & n^{-} \end{pmatrix}. \quad (2.34)$$

The Minkowski metric in the null basis has the form

$$(g_{\mu\nu}) = \frac{1}{2} \begin{pmatrix} 0 & 1 & 0 & 0 \\ 1 & 0 & 0 & 0 \\ 0 & 0 & 0 & -1 \\ 0 & 0 & -1 & 0 \end{pmatrix}, \quad (g^{\mu\nu}) = 2 \begin{pmatrix} 0 & 1 & 0 & 0 \\ 1 & 0 & 0 & 0 \\ 0 & 0 & 0 & -1 \\ 0 & 0 & -1 & 0 \end{pmatrix}. \quad (2.35)$$

We note that for real vectors $n^{\bar{\perp}} = \overline{n^{\perp}}$, but for complex vectors, we have $n^{\bar{\perp}} = \overline{\bar{n}^{\perp}}$

$$\bar{n}^{\mu} = \begin{pmatrix} \bar{n}^{+} & \bar{n}^{-} & \bar{n}^{\perp} & \bar{n}^{\bar{\perp}} \end{pmatrix}^{\mu} = \begin{pmatrix} \overline{n^{+}} & \overline{n^{-}} & \overline{n^{\perp}} & \overline{n^{\bar{\perp}}} \end{pmatrix}^{\mu}. \quad (2.36)$$

We choose the basis spinors to be

$$o_A = \begin{pmatrix} 0 \\ 1 \end{pmatrix}, \quad \iota_A = \begin{pmatrix} -1 \\ 0 \end{pmatrix}, \quad o^A = \varepsilon^{AB} o_B = \begin{pmatrix} 1 \\ 0 \end{pmatrix}, \quad \iota^A = \varepsilon^{AB} \iota_B = \begin{pmatrix} 0 \\ 1 \end{pmatrix}, \quad (2.37)$$

thus the symplectic form in the matrix form is

$$\varepsilon_{AB} = o_A \iota_B - \iota_A o_B = \begin{pmatrix} 0 & 1 \\ -1 & 0 \end{pmatrix} = \varepsilon^{AB} = o^A \iota^B - \iota^A o^B. \quad (2.38)$$

With this choice of spinor basis, we define the bispinor basis

$$\begin{aligned} |\uparrow\rangle &= \begin{bmatrix} o_A \\ 0 \end{bmatrix} = \begin{bmatrix} 0 \\ 1 \\ 0 \\ 0 \end{bmatrix}, & |\uparrow\rangle &= \begin{bmatrix} 0 \\ \bar{o}_{\dot{A}} \end{bmatrix} = \begin{bmatrix} 0 \\ 0 \\ 1 \\ 0 \end{bmatrix}, \\ |\downarrow\rangle &= \begin{bmatrix} \iota_A \\ 0 \end{bmatrix} = \begin{bmatrix} -1 \\ 0 \\ 0 \\ 0 \end{bmatrix}, & |\downarrow\rangle &= \begin{bmatrix} 0 \\ \bar{\iota}_{\dot{A}} \end{bmatrix} = \begin{bmatrix} 0 \\ 0 \\ 0 \\ 1 \end{bmatrix}, \\ \langle\uparrow| &= [o^A \quad 0] = [1 \quad 0 \quad 0 \quad 0], & \langle\uparrow| &= [0 \quad \bar{o}_{\dot{A}}] = [0 \quad 0 \quad 0 \quad 1], \\ \langle\downarrow| &= [\iota^A \quad 0] = [0 \quad 1 \quad 0 \quad 0], & \langle\downarrow| &= [0 \quad \bar{\iota}_{\dot{A}}] = [0 \quad 0 \quad -1 \quad 0]. \end{aligned} \quad (2.39)$$

From this basis, one can check by explicit calculation that for the basis vectors (2.9), we have the completeness relation

$$\widehat{l}_+ = |\uparrow\rangle [\uparrow| + |\uparrow\rangle \langle\uparrow|, \quad [\uparrow| \gamma^\mu |\uparrow\rangle = 2l_+^\mu, \quad (2.40a)$$

$$\widehat{l}_- = |\downarrow\rangle [\downarrow| + |\downarrow\rangle \langle\downarrow|, \quad [\downarrow| \gamma^\mu |\downarrow\rangle = 2l_-^\mu, \quad (2.40b)$$

$$\widehat{m} = |\downarrow\rangle [\uparrow| + |\uparrow\rangle \langle\downarrow|, \quad [\uparrow| \gamma^\mu |\downarrow\rangle = 2m^\mu, \quad (2.40c)$$

$$\widehat{\bar{m}} = |\uparrow\rangle [\downarrow| + |\downarrow\rangle \langle\uparrow|, \quad [\downarrow| \gamma^\mu |\uparrow\rangle = 2\bar{m}^\mu. \quad (2.40d)$$

Using the bispinor basis, we can write also the completeness relations in eigenspaces of chirality

$$P_\pm = \frac{1 \pm \gamma_5}{2}, \quad P_+ = |\downarrow\rangle \langle\uparrow| - |\uparrow\rangle \langle\downarrow|, \quad P_- = |\uparrow\rangle \langle\downarrow| - |\downarrow\rangle \langle\uparrow|. \quad (2.41)$$

Let us choose the reference spinor ρ^A to be ι^A . Then we have $l = l_-$ and $2(p \cdot l) = p^+$. The Weyl spinors $\theta(p)_A$ used to construct solutions of the Dirac equation take the form

$$\theta(p)_A = \frac{p_{A\dot{1}}}{\sqrt{|p^+|}} = \frac{1}{\sqrt{|p^+|}} (p^+ o_A + p^\perp \iota_A) = \frac{1}{\sqrt{|p^+|}} \begin{pmatrix} -p^\perp \\ p^+ \end{pmatrix}. \quad (2.42)$$

Therefore, the corresponding bispinor brackets are

$$\begin{aligned} |p] &= \frac{1}{\sqrt{|p^+|}} \left(p^+ |\uparrow\rangle + p^\perp |\downarrow\rangle + m |\downarrow\rangle \right), \\ |p\rangle &= \frac{1}{\sqrt{|p^+|}} \left(p^+ |\uparrow\rangle + p^\perp |\downarrow\rangle - m |\downarrow\rangle \right). \end{aligned} \quad (2.43)$$

3. Amplitudes

3.1. Derivation of the amplitudes

The amplitude for the $g^*g^* \rightarrow \bar{q}qV^*$ scattering at the tree level is given by diagrams presented in figure 2. Some care is needed to define the amplitude involving off-shell gluons in a gauge-invariant way, *e.g.* by embedding as a subprocess in an on-shell process of scattering of two fast quarks [15, 16, 22]. This leads to a replacement of the ordinary QCD three-gluon vertex with the so-called Lipatov vertex [24] (defined in (3.11) below), which, apart from the standard ggg interaction in QCD, takes into account an exchange of gluon between the two quarks and gluon radiation.

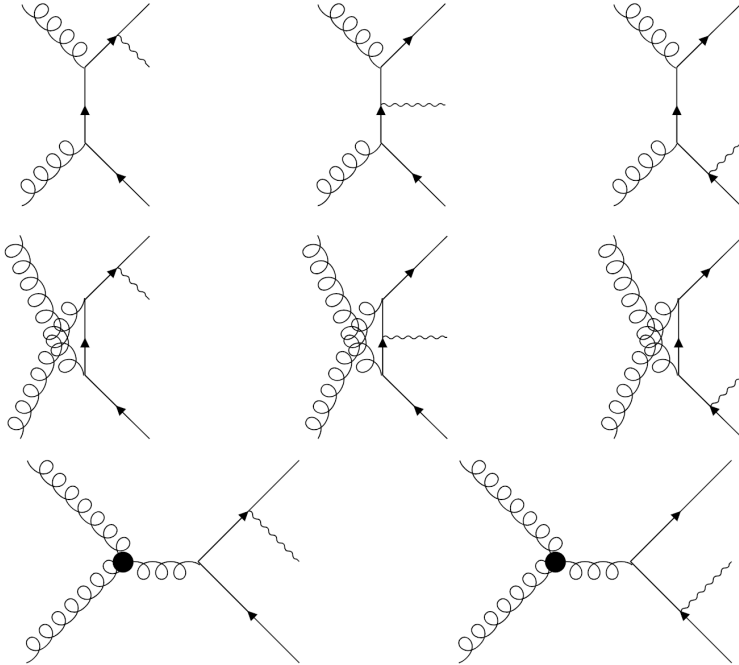


Fig. 2. Eight Feynman diagrams describing the $g^*g^* \rightarrow \bar{q}qV^*$ scattering at the tree level. The bold dot represents the Lipatov vertex.

We take the vertex of interaction with the boson V^* to be

$$\Gamma^\mu = v\gamma^\mu + a\gamma_5\gamma^\mu. \quad (3.1)$$

For example, if $V^* = \gamma^*$ (excited photon), then $v = e_f$ and $a = 0$. We need the more general vertex to treat the W and Z bosons. We denote colors of the ingoing gluons by a, b . The $q\bar{q}$ pair is taken to have colors i, j , and spins σ_3, σ_4 . The contributions to the amplitude from the eight diagrams take the following forms:

$$\begin{aligned} \mathcal{A}_1^\mu &= \frac{-ig^2}{(v_1^2 - m_4^2)(v_2^2 - m_4^2)} \left(T^a T^b\right)_{ij} \\ &\quad \times \bar{u}_{\sigma_3}(p_3) \Gamma^\mu (\hat{v}_1 + m_4) \hat{P}_1 (\hat{v}_2 + m_4) \hat{P}_2 v_{\sigma_4}(p_4) \\ &=: -ig^2 \left(T^a T^b\right)_{ij} A_1^\mu, \end{aligned} \quad (3.2)$$

$$\begin{aligned} \mathcal{A}_2^\mu &= \frac{-ig^2}{(v_3^2 - m_3^2)(v_2^2 - m_4^2)} \left(T^a T^b\right)_{ij} \\ &\quad \times \bar{u}_{\sigma_3}(p_3) \hat{P}_1 (\hat{v}_3 + m_3) \Gamma^\mu (\hat{v}_2 + m_4) \hat{P}_2 v_{\sigma_4}(p_4) \\ &=: -ig^2 \left(T^a T^b\right)_{ij} A_2^\mu, \end{aligned} \quad (3.3)$$

$$\begin{aligned} \mathcal{A}_3^\mu &= \frac{-ig^2}{(v_3^2 - m_3^2)(v_4^2 - m_3^2)} \left(T^a T^b\right)_{ij} \\ &\quad \times \bar{u}_{\sigma_3}(p_3) \hat{P}_1 (\hat{v}_3 + m_3) \hat{P}_2 (\hat{v}_4 + m_3) \Gamma^\mu v_{\sigma_4}(p_4) \\ &=: -ig^2 \left(T^a T^b\right)_{ij} A_3^\mu, \end{aligned} \quad (3.4)$$

$$\begin{aligned} \mathcal{A}_4^\mu &= \frac{-ig^2}{(v_1^2 - m_4^2)(v_5^2 - m_4^2)} \left(T^b T^a\right)_{ij} \\ &\quad \times \bar{u}_{\sigma_3}(p_3) \Gamma^\mu (\hat{v}_1 + m_4) \hat{P}_2 (\hat{v}_5 + m_4) \hat{P}_1 v_{\sigma_4}(p_4) \\ &=: -ig^2 \left(T^b T^a\right)_{ij} A_4^\mu, \end{aligned} \quad (3.5)$$

$$\begin{aligned} \mathcal{A}_5^\mu &= \frac{-ig^2}{(v_6^2 - m_3^2)(v_5^2 - m_4^2)} \left(T^b T^a\right)_{ij} \\ &\quad \times \bar{u}_{\sigma_3}(p_3) \hat{P}_2 (\hat{v}_6 + m_3) \Gamma^\mu (\hat{v}_5 + m_4) \hat{P}_1 v_{\sigma_4}(p_4) \\ &=: -ig^2 \left(T^b T^a\right)_{ij} A_5^\mu, \end{aligned} \quad (3.6)$$

$$\begin{aligned}
\mathcal{A}_6^\mu &= \frac{-ig^2}{(v_4^2 - m_3^2)(v_6^2 - m_3^2)} \left(T^b T^a\right)_{ij} \\
&\quad \times \bar{u}_{\sigma_3}(p_3) \hat{P}_2(\hat{v}_6 + m_3) \hat{P}_1(\hat{v}_4 + m_3) \Gamma^\mu v_{\sigma_4}(p_4) \\
&=: -ig^2 \left(T^b T^a\right)_{ij} A_6^\mu,
\end{aligned} \tag{3.7}$$

$$\begin{aligned}
\mathcal{A}_7^\mu &= \frac{g^2}{(k_1 + k_2)^2 (v_1^2 - m_4^2)} f^{abc} T_{ij}^c \bar{u}_{\sigma_3}(p_3) \Gamma^\mu (\hat{v}_1 + m_4) \hat{V}_{\text{eff}} v_{\sigma_4}(p_4) \\
&=: g^2 f^{abc} T_{ij}^c A_7^\mu,
\end{aligned} \tag{3.8}$$

$$\begin{aligned}
\mathcal{A}_8^\mu &= \frac{g^2}{(k_1 + k_2)^2 (v_4^2 - m_3^2)} f^{abc} T_{ij}^c \bar{u}_{\sigma_3}(p_3) \hat{V}_{\text{eff}} (\hat{v}_4 + m_3) \Gamma^\mu v_{\sigma_4}(p_4) \\
&=: g^2 f^{abc} T_{ij}^c A_8^\mu,
\end{aligned} \tag{3.9}$$

where v_i are momenta flowing in internal lines

$$\begin{aligned}
v_1 &= p_3 + q, & v_2 &= k_2 - p_4, & v_3 &= p_3 - k_1, \\
v_4 &= -p_4 - q, & v_5 &= k_1 - p_4, & v_6 &= p_3 - k_2,
\end{aligned} \tag{3.10}$$

and the form of V_{eff}^μ results from the contraction of the Lipatov vertex with the approximated gluon polarizations:

$$\begin{aligned}
V_{\text{eff}}^\mu &= \frac{S}{2} (k_2 - k_1)^\mu + \left(2P_2 \cdot k_1 + \frac{P_1 \cdot P_2}{P_1 \cdot k_2} k_1^2 \right) P_1^\mu \\
&\quad - \left(2P_1 \cdot k_2 + \frac{P_1 \cdot P_2}{P_2 \cdot k_1} k_2^2 \right) P_2^\mu \\
&= \frac{S}{2} (k_2 - k_1)^\mu + \left(x_1 S + \frac{k_1^2}{x_2} \right) P_1^\mu - \left(x_2 S + \frac{k_2^2}{x_1} \right) P_2^\mu.
\end{aligned} \tag{3.11}$$

We have factorized the amplitudes \mathcal{A}_i^μ into color factors and color-independent amplitudes A_i^μ . The full amplitude can be decomposed into parts symmetric and antisymmetric in the color indices a, b

$$\mathcal{A}^\mu := \sum_{n=1}^8 \mathcal{A}_n^\mu = \mathcal{A}_S^\mu + \mathcal{A}_A^\mu, \tag{3.12}$$

where

$$\begin{aligned}
\mathcal{A}_S^\mu &:= -ig^2 \left(\frac{1}{N} \delta^{ab} \delta_{ij} + d^{abc} T_{ij}^c \right) A_S^\mu, \\
\mathcal{A}_A^\mu &:= g^2 f^{abc} T_{ij}^c A_A^\mu.
\end{aligned} \tag{3.13}$$

and

$$A_S^\mu := \frac{1}{2} \sum_{n=1}^6 A_n^\mu, \quad A_A^\mu := \frac{1}{2} (A_1^\mu + A_2^\mu + A_3^\mu - A_4^\mu - A_5^\mu - A_6^\mu) + A_7^\mu + A_8^\mu. \quad (3.14)$$

In the amplitude squared, averaged over colors of the ingoing gluons, and summed over colors of the outgoing $q\bar{q}$, the symmetric and antisymmetric parts do not interfere

$$\begin{aligned} \mathcal{M}^{\mu\nu} &= \frac{1}{(N^2 - 1)^2} \sum_{i,j,a,b} \mathcal{A}^\mu \bar{\mathcal{A}}^\nu \\ &= \frac{1}{(N^2 - 1)^2} \sum_{i,j,a,b} \mathcal{A}_S^\mu \bar{\mathcal{A}}_S^\nu + \frac{1}{(N^2 - 1)^2} \sum_{i,j,a,b} \mathcal{A}_A^\mu \bar{\mathcal{A}}_A^\nu \\ &= \frac{g^4 (N^2 - 2)}{2N (N^2 - 1)} A_S^\mu \bar{A}_S^\nu + \frac{g^4 N}{2 (N^2 - 1)} A_A^\mu \bar{A}_A^\nu = \mathcal{M}_S^{\mu\nu} + \mathcal{M}_A^{\mu\nu}. \end{aligned} \quad (3.15)$$

We can further decompose each amplitude into right R^μ and left L^μ part

$$A_n^\mu = (v + a)R_n^\mu + (v - a)L_n^\mu, \quad (3.16)$$

where in R_i^μ we replace Γ^μ by $P_+ \gamma^\mu$ and in L_i^μ we replace Γ^μ by $P_- \gamma^\mu$.

In the brackets notation, we put for fermions

$$u_+(p) = |p\rangle, \quad u_-(p) = |p], \quad \bar{u}_+(p) = [p|, \quad \bar{u}_-(p) = \langle p|, \quad (3.17)$$

and for antifermions

$$v_-(p) = |-p\rangle, \quad v_+(p) = |-p], \quad \bar{v}_-(p) = [-p|, \quad \bar{v}_+(p) = \langle -p|, \quad (3.18)$$

with brackets defined as in Section 2. In the massless case, the indices \pm refer to helicity (so they agree with chirality for the quark and are opposite to chirality for the antiquark). For massive particles, $\pm \frac{1}{2}$ is minus the spin in the rest frame of p projected onto the spatial direction of l_- . Equivalently, they are eigenvectors of the spin operator S_p as described in (2.22) (where we have to keep in mind that for antiparticles, the physical spin is opposite to the spin operator from Dirac's theory).

3.2. Results in the massless case

In the massless case we encounter a huge simplification, so there is a good reason to consider it separately. Firstly, amplitudes with fermions of the same chirality vanish

$$A_{n,+ -}^\mu = 0 = A_{n,- +}^\mu. \quad (3.19)$$

The nonzero amplitudes are given as

$$A_{n,++}^\mu = (v+a)R_{n,++}^\mu \quad \text{and} \quad A_{n,--}^\mu = (v-a)L_{n,--}^\mu. \quad (3.20)$$

Below, we give formulas only for $R_{n,+ -}$. Other amplitudes may be reconstructed from the following symmetry:

$$L_{n,--}^\mu = \bar{R}_{n,++}^\mu, \quad (3.21)$$

which is the consequence of the symmetries (2.30) and (2.31).

We obtained the following results for $R_{n,+ -}^\mu$:

$$\begin{aligned} R_{1,++}^{\dot{A}A} &= \langle p_3 | \gamma^{\dot{A}A} \frac{\hat{v}_1}{v_1^2} \hat{P}_1 \frac{\hat{v}_2}{v_2^2} \hat{P}_2 | -p_4 \rangle = -\frac{2S}{v_1^2 v_2^2 \sqrt{p_3^+ p_4^+}} p_4^{\dot{0}0} v_2^{\dot{0}1} p_3^{\dot{A}0} v_1^{\dot{1}A}, \\ R_{2,++}^{\dot{A}A} &= \langle p_3 | \hat{P}_1 \frac{\hat{v}_3}{v_3^2} \gamma^{\dot{A}A} \frac{\hat{v}_2}{v_2^2} \hat{P}_2 | -p_4 \rangle = -\frac{2S}{v_3^2 v_2^2 \sqrt{p_3^+ p_4^+}} p_4^{\dot{0}0} p_3^{\dot{1}0} v_3^{\dot{A}1} v_2^{\dot{0}A}, \\ R_{3,++}^{\dot{A}A} &= \langle p_3 | \hat{P}_1 \frac{\hat{v}_3}{v_3^2} \hat{P}_2 \frac{\hat{v}_4}{v_4^2} \gamma^{\dot{A}A} | -p_4 \rangle = -\frac{2S}{v_3^2 v_4^2 \sqrt{p_3^+ p_4^+}} p_3^{\dot{1}0} v_3^{\dot{0}1} v_4^{\dot{A}0} p_4^{\dot{0}A}, \\ R_{4,++}^{\dot{A}A} &= \langle p_3 | \gamma^{\dot{A}A} \frac{\hat{v}_1}{v_1^2} \hat{P}_2 \frac{\hat{v}_5}{v_5^2} \hat{P}_1 | -p_4 \rangle = -\frac{2S}{v_1^2 v_5^2 \sqrt{p_3^+ p_4^+}} p_4^{\dot{0}1} v_5^{\dot{1}0} p_3^{\dot{A}0} v_1^{\dot{0}A}, \\ R_{5,++}^{\dot{A}A} &= \langle p_3 | \hat{P}_2 \frac{\hat{v}_6}{v_6^2} \gamma^{\dot{A}A} \frac{\hat{v}_5}{v_5^2} \hat{P}_1 | -p_4 \rangle = -\frac{2S}{v_6^2 v_5^2 \sqrt{p_3^+ p_4^+}} p_3^{\dot{0}0} p_4^{\dot{0}1} v_6^{\dot{A}0} v_5^{\dot{1}A}, \\ R_{6,++}^{\dot{A}A} &= \langle p_3 | \hat{P}_2 \frac{\hat{v}_6}{v_6^2} \hat{P}_1 \frac{\hat{v}_4}{v_4^2} \gamma^{\dot{A}A} | -p_4 \rangle = -\frac{2S}{v_6^2 v_4^2 \sqrt{p_3^+ p_4^+}} p_3^{\dot{0}0} v_6^{\dot{1}0} v_4^{\dot{A}1} p_4^{\dot{0}A}, \\ R_{7,++}^{\dot{A}A} &= \frac{1}{(k_1 + k_2)^2} \langle p_3 | \gamma^{\dot{A}A} \frac{\hat{v}_1}{v_1^2} \hat{V}_{\text{eff}} | -p_4 \rangle \\ &= -\frac{2}{v_1^2 (k_1 + k_2)^2 \sqrt{p_3^+ p_4^+}} p_3^{\dot{A}0} p_4^{\dot{0}B} (V_{\text{eff}})_{B\dot{B}} v_1^{\dot{B}A}, \\ R_{8,++}^{\dot{A}A} &= \frac{1}{(k_1 + k_2)^2} \langle p_3 | \hat{V}_{\text{eff}} \frac{\hat{v}_4}{v_4^2} \gamma^{\dot{A}A} | -p_4 \rangle \\ &= -\frac{2}{v_4^2 (k_1 + k_2)^2 \sqrt{p_3^+ p_4^+}} v_4^{\dot{A}B} (V_{\text{eff}})_{B\dot{B}} p_3^{\dot{B}0} p_4^{\dot{0}A}. \end{aligned} \quad (3.22)$$

These results take the simplest forms in terms of the spinor notation, but as an example, we give two formulas written in Lorentz vector notation

$$R_{1,++}^\mu = -\frac{2S}{v_1^2 v_2^2} \sqrt{\frac{p_4^+}{p_3^+}} v_2^\perp (p_3^+ v_1^\perp \quad p_3^\perp v_1^- \quad p_3^\perp v_1^\perp \quad p_3^+ v_1^-)^\mu, \quad (3.23)$$

$$R_{7,++}^\mu = -\frac{4}{v_1^2 (k_1 + k_2)^2 \sqrt{p_3^+ p_4^+}} M_7^{\mu\nu} (V_{\text{eff}})_\nu, \quad (3.24)$$

where M_7 is the following matrix:

$$M_7^{\mu\nu} = \begin{pmatrix} p_3^+ p_4^+ v_1^\perp & p_3^+ p_4^\perp v_1^\perp & p_3^\perp p_4^+ v_1^\perp & p_3^\perp p_4^\perp v_1^\perp \\ p_3^\perp p_4^+ v_1^\perp & p_3^\perp p_4^\perp v_1^\perp & p_3^\perp p_4^+ v_1^- & p_3^\perp p_4^\perp v_1^- \\ p_3^\perp p_4^+ v_1^\perp & p_3^\perp p_4^\perp v_1^\perp & p_3^\perp p_4^+ v_1^\perp & p_3^\perp p_4^\perp v_1^\perp \\ p_3^+ p_4^+ v_1^\perp & p_3^+ p_4^\perp v_1^- & p_3^+ p_4^+ v_1^- & p_3^+ p_4^\perp v_1^\perp \end{pmatrix}^{\mu\nu}. \quad (3.25)$$

We remark that the simple structure of amplitudes written in terms of spinors is reflected in the fact that M_7 is a matrix of rank at most 2.

3.3. General results

In the massive case, we have 8 expressions to compute for each diagram: left and right amplitudes with two possible values of spin for the quark and for antiquark. In contrast to the massless case none of these expressions vanish identically, but we can still reduce the number of independent amplitudes by a factor of two using the symmetries

$$\begin{aligned} R_{n,-+}^\mu &= \bar{L}_{n,+}^\mu, & L_{n,-+}^\mu &= \bar{R}_{n,+}^\mu, \\ R_{n,--}^\mu &= -\bar{L}_{n,++}^\mu, & L_{n,--}^\mu &= -\bar{R}_{n,++}^\mu, \end{aligned} \quad (3.26)$$

which, similarly like in the massless case, are reflection of symmetries (2.30) and (2.31). Therefore, for each diagram, we write only $R_{n,++}^\mu, L_{n,++}^\mu, R_{n,+-}^\mu$ and $L_{n,+-}^\mu$.

The first diagram

$$\begin{aligned} R_{1,++}^{AA} &= -\frac{2S}{(v_1^2 - m_4^2)(v_2^2 - m_4^2)} \frac{p_4^{\dot{0}0} p_3^{\dot{A}0}}{\sqrt{p_3^+ p_4^+}} \left[v_2^{\dot{0}1} v_1^{\dot{1}A} + m_4^2 o^A \right], \\ L_{1,++}^{AA} &= -\frac{2S}{(v_1^2 - m_4^2)(v_2^2 - m_4^2)} \frac{m_3 m_4 p_4^{\dot{0}0}}{\sqrt{p_3^+ p_4^+}} \left[v_1^{\dot{A}1} + v_2^{\dot{0}1} \bar{o}^{\dot{A}} \right] \iota^A, \end{aligned} \quad (3.27)$$

$$\begin{aligned}
R_{1,+ -}^{\dot{A}A} &= -\frac{2S}{(v_1^2 - m_4^2)(v_2^2 - m_4^2)} \frac{m_4 p_4^{\dot{0}0} p_3^{\dot{A}0}}{\sqrt{p_3^+ p_4^+}} \left[v_2^{\dot{1}0} o^A - v_1^{\dot{1}A} \right], \\
L_{1,+ -}^{\dot{A}A} &= -\frac{2S}{(v_1^2 - m_4^2)(v_2^2 - m_4^2)} \frac{m_3 p_4^{\dot{0}0}}{\sqrt{p_3^+ p_4^+}} \left[v_2^{\dot{1}0} v_1^{\dot{A}1} + m_4^2 \bar{o}^{\dot{A}} \right] \iota^A. \quad (3.28)
\end{aligned}$$

The second diagram

$$\begin{aligned}
R_{2,++}^{\dot{A}A} &= -\frac{2S}{(v_3^2 - m_3^2)(v_2^2 - m_4^2)} \frac{p_4^{\dot{0}0}}{\sqrt{p_3^+ p_4^+}} \left[p_3^{\dot{1}0} v_3^{\dot{A}1} + m_3^2 \bar{o}^{\dot{A}} \right] v_2^{\dot{0}A}, \\
L_{2,++}^{\dot{A}A} &= -\frac{2S}{(v_3^2 - m_3^2)(v_2^2 - m_4^2)} \frac{m_3 m_4 p_4^{\dot{0}0}}{\sqrt{p_3^+ p_4^+}} \left[v_3^{\dot{A}1} + v_2^{\dot{0}1} \bar{o}^{\dot{A}} \right] \bar{\iota}^{\dot{A}}, \quad (3.29)
\end{aligned}$$

$$\begin{aligned}
R_{2,+ -}^{\dot{A}A} &= \frac{2S}{(v_3^2 - m_3^2)(v_2^2 - m_4^2)} \frac{m_4 p_4^{\dot{0}0}}{\sqrt{p_3^+ p_4^+}} \left[p_3^{\dot{1}0} v_3^{\dot{A}1} + m_3^2 \bar{o}^{\dot{A}} \right] \iota^A, \\
L_{2,+ -}^{\dot{A}A} &= -\frac{2S}{(v_3^2 - m_3^2)(v_2^2 - m_4^2)} \frac{m_3 p_4^{\dot{0}0}}{\sqrt{p_3^+ p_4^+}} \left[v_3^{\dot{1}A} - p_3^{\dot{1}0} o^A \right] v_2^{\dot{A}0}. \quad (3.30)
\end{aligned}$$

The third diagram

$$\begin{aligned}
R_{3,++}^{\dot{A}A} &= -\frac{2S}{(v_3^2 - m_3^2)(v_4^2 - m_3^2)} \frac{p_4^{\dot{0}A}}{\sqrt{p_3^+ p_4^+}} \\
&\quad \times \left[p_3^{\dot{1}0} v_3^{\dot{0}1} v_4^{\dot{A}0} + m_3^2 \left((p_3 - v_3)^{\dot{1}0} \bar{\iota}^{\dot{A}} + v_4^{\dot{A}0} \right) \right] v_2^{\dot{0}A}, \\
L_{3,++}^{\dot{A}A} &= \frac{2S}{(v_3^2 - m_3^2)(v_4^2 - m_3^2)} \frac{m_3 m_4}{\sqrt{p_3^+ p_4^+}} \\
&\quad \times \left[\left(m_3^2 + p_3^{\dot{1}0} v_3^{\dot{0}1} \right) \iota^A - (p_3 - v_3)^{\dot{1}0} v_4^{\dot{0}A} \right] \bar{\iota}^{\dot{A}}, \quad (3.31)
\end{aligned}$$

$$\begin{aligned}
R_{3,+ -}^{\dot{A}A} &= -\frac{2S}{(v_3^2 - m_3^2)(v_4^2 - m_3^2)} \frac{m_4}{\sqrt{p_3^+ p_4^+}} \\
&\quad \times \left[\left(m_3^2 + p_3^{\dot{1}0} v_3^{\dot{0}1} \right) v_4^{\dot{A}1} + m_3^2 (p_3 - v_3)^{\dot{1}0} \bar{\iota}^{\dot{A}} \right] \iota^A, \\
L_{3,+ -}^{\dot{A}A} &= -\frac{2S}{(v_3^2 - m_3^2)(v_4^2 - m_3^2)} \frac{m_3 p_4^{\dot{0}0}}{\sqrt{p_3^+ p_4^+}} \\
&\quad \times \left[\left(m_3^2 + p_3^{\dot{1}0} v_3^{\dot{0}1} \right) \iota^A - (p_3 - v_3)^{\dot{1}0} v_4^{\dot{0}A} \right]. \tag{3.32}
\end{aligned}$$

The fourth diagram

$$\begin{aligned}
R_{4,++}^{\dot{A}A} &= \frac{2S}{(v_1^2 - m_4^2)(v_5^2 - m_4^2)} \frac{p_3^{\dot{A}0}}{\sqrt{p_3^+ p_4^+}} \\
&\quad \times \left[\left(m_4^2 - p_4^{\dot{0}1} v_5^{\dot{1}0} \right) v_1^{\dot{A}0} - m_4^2 (p_4 + v_5)^{\dot{0}1} \iota^A \right], \\
L_{4,++}^{\dot{A}A} &= \frac{2S}{(v_1^2 - m_4^2)(v_5^2 - m_4^2)} \frac{m_3 m_4}{\sqrt{p_3^+ p_4^+}} \\
&\quad \times \left[\left(m_4^2 - p_4^{\dot{0}1} v_5^{\dot{1}0} \right) \bar{\iota}^{\dot{A}} + (p_4 + v_5)^{\dot{0}1} v_1^{\dot{A}0} \right] \iota^A, \tag{3.33}
\end{aligned}$$

$$\begin{aligned}
R_{4,+ -}^{\dot{A}A} &= -\frac{2S}{(v_1^2 - m_4^2)(v_5^2 - m_4^2)} \frac{m_4 p_3^{\dot{A}0}}{\sqrt{p_3^+ p_4^+}} \\
&\quad \times \left[\left(m_4^2 - p_4^{\dot{1}0} v_5^{\dot{0}1} \right) \iota^A + m_3^2 (p_4 + v_5)^{\dot{1}0} v_1^{\dot{0}A} \right], \\
L_{4,+ -}^{\dot{A}A} &= \frac{2S}{(v_1^2 - m_4^2)(v_5^2 - m_4^2)} \frac{m_3}{\sqrt{p_3^+ p_4^+}} \\
&\quad \times \left[\left(m_4^2 - p_4^{\dot{1}0} v_5^{\dot{0}1} \right) v_1^{\dot{A}0} - (p_4 + v_5)^{\dot{1}0} \bar{\iota}^{\dot{A}} \right] \iota^A. \tag{3.34}
\end{aligned}$$

The fifth diagram

$$\begin{aligned}
R_{5,++}^{\dot{A}A} &= \frac{2S}{(v_6^2 - m_3^2)(v_5^2 - m_4^2)} \frac{p_3^{\dot{0}0}}{\sqrt{p_3^+ p_4^+}} \left[m_4^2 o^A - p_4^{\dot{0}1} v_5^{\dot{1}A} \right] v_6^{\dot{A}0}, \\
L_{5,++}^{\dot{A}A} &= \frac{2S}{(v_6^2 - m_3^2)(v_5^2 - m_4^2)} \frac{m_3 m_4 p_3^{\dot{0}0}}{\sqrt{p_3^+ p_4^+}} \left[v_5^{\dot{A}1} + p_4^{\dot{0}1} \bar{o}^{\dot{A}} \right] \iota^A, \tag{3.35}
\end{aligned}$$

$$\begin{aligned}
R_{5,+}^{\dot{A}\dot{A}} &= -\frac{2S}{(v_6^2 - m_3^2)(v_5^2 - m_4^2)} \frac{m_4 p_3^{\dot{0}\dot{0}}}{\sqrt{p_3^+ p_4^+}} \left[v_5^{\dot{1}\dot{A}} + p_4^{\dot{1}\dot{0}} o^{\dot{A}} \right] v_6^{\dot{A}\dot{0}}, \\
L_{5,+}^{\dot{A}\dot{A}} &= -\frac{2S}{(v_6^2 - m_3^2)(v_5^2 - m_4^2)} \frac{m_3 p_3^{\dot{0}\dot{0}}}{\sqrt{p_3^+ p_4^+}} \left[m_4^2 \bar{o}^{\dot{A}} - p_4^{\dot{1}\dot{0}} v_5^{\dot{A}\dot{1}} \right] \iota^{\dot{A}}. \quad (3.36)
\end{aligned}$$

The sixth diagram

$$\begin{aligned}
R_{6,++}^{\dot{A}\dot{A}} &= -\frac{2S}{(v_6^2 - m_3^2)(v_4^2 - m_3^2)} \frac{p_3^{\dot{0}\dot{0}} p_4^{\dot{0}\dot{A}}}{\sqrt{p_3^+ p_4^+}} \left[v_6^{\dot{1}\dot{0}} v_4^{\dot{A}\dot{1}} + m_3^2 \bar{o}^{\dot{A}} \right], \\
L_{6,++}^{\dot{A}\dot{A}} &= \frac{2S}{(v_6^2 - m_3^2)(v_4^2 - m_3^2)} \frac{m_3 m_4 p_3^{\dot{0}\dot{0}}}{\sqrt{p_3^+ p_4^+}} \left[v_4^{\dot{1}\dot{A}} - v_6^{\dot{1}\dot{0}} o^{\dot{A}} \right] \bar{\iota}^{\dot{A}}, \quad (3.37)
\end{aligned}$$

$$\begin{aligned}
R_{6,+}^{\dot{A}\dot{A}} &= -\frac{2S}{(v_6^2 - m_3^2)(v_4^2 - m_3^2)} \frac{m_4 p_3^{\dot{0}\dot{0}}}{\sqrt{p_3^+ p_4^+}} \left[v_4^{\dot{A}\dot{1}} v_6^{\dot{1}\dot{0}} + m_3^2 \bar{o}^{\dot{A}} \right] \iota^{\dot{A}}, \\
L_{6,+}^{\dot{A}\dot{A}} &= \frac{2S}{(v_6^2 - m_3^2)(v_4^2 - m_3^2)} \frac{m_3 p_3^{\dot{0}\dot{0}} p_4^{\dot{A}\dot{0}}}{\sqrt{p_3^+ p_4^+}} \left[v_6^{\dot{1}\dot{0}} o^{\dot{A}} - v_4^{\dot{1}\dot{A}} \right]. \quad (3.38)
\end{aligned}$$

The seventh diagram

$$\begin{aligned}
R_{7,++}^{\dot{A}\dot{A}} &= \frac{2}{(v_1^2 - m_4^2)(k_1 + k_2)^2} \frac{p_3^{\dot{A}\dot{0}}}{\sqrt{p_3^+ p_4^+}} \\
&\quad \times \left[-p_4^{\dot{0}\dot{B}} (V_{\text{eff}})_{B\dot{B}} v_1^{\dot{B}\dot{A}} + m_4^2 (V_{\text{eff}})^{\dot{0}\dot{A}} \right], \\
L_{7,++}^{\dot{A}\dot{A}} &= -\frac{2}{(v_1^2 - m_4^2)(k_1 + k_2)^2} \frac{m_3 m_4 \varepsilon_{BC}}{\sqrt{p_3^+ p_4^+}} \\
&\quad \times \left[v_1^{\dot{A}\dot{B}} (V_{\text{eff}})^{\dot{0}\dot{C}} - (V_{\text{eff}})^{\dot{A}\dot{B}} p_4^{\dot{0}\dot{C}} \right] \iota^{\dot{A}}, \quad (3.39)
\end{aligned}$$

$$\begin{aligned}
R_{7,+}^{\dot{A}\dot{A}} &= \frac{2}{(v_1^2 - m_4^2)(k_1 + k_2)^2} \frac{m_4 p_3^{\dot{A}\dot{0}} \varepsilon_{\dot{B}\dot{C}}}{\sqrt{p_3^+ p_4^+}} \left[v_1^{\dot{B}\dot{A}} (V_{\text{eff}})^{\dot{C}\dot{0}} - (V_{\text{eff}})^{\dot{B}\dot{A}} p_4^{\dot{C}\dot{0}} \right], \\
L_{7,+}^{\dot{A}\dot{A}} &= \frac{2}{(v_1^2 - m_4^2)(k_1 + k_2)^2} \frac{m_3}{\sqrt{p_3^+ p_4^+}} \\
&\quad \times \left[-v_1^{\dot{A}\dot{B}} (V_{\text{eff}})_{B\dot{B}} p_4^{\dot{B}\dot{0}} + m_4^2 (V_{\text{eff}})^{\dot{A}\dot{0}} \right] \iota^{\dot{A}}. \quad (3.40)
\end{aligned}$$

The eighth diagram

$$\begin{aligned}
 R_{8,++}^{\dot{A}A} &= -\frac{2}{(v_4^2 - m_3^2)(k_1 + k_2)^2} \frac{p_4^{\dot{0}A}}{\sqrt{p_3^+ p_4^+}} \\
 &\quad \times \left[v_4^{\dot{A}B} (V_{\text{eff}})_{B\dot{B}} p_3^{\dot{B}0} + m_3^2 (V_{\text{eff}})^{\dot{A}0} \right], \\
 L_{8,++}^{\dot{A}A} &= -\frac{2}{(v_4^2 - m_3^2)(k_1 + k_2)^2} \frac{m_3 m_4 \varepsilon_{\dot{B}\dot{C}}}{\sqrt{p_3^+ p_4^+}} \\
 &\quad \times \left[v_4^{\dot{B}A} (V_{\text{eff}})^{\dot{C}0} + (V_{\text{eff}})^{\dot{B}A} p_3^{\dot{C}0} \right] \bar{t}^{\dot{A}}, \tag{3.41}
 \end{aligned}$$

$$\begin{aligned}
 R_{8,+-}^{\dot{A}A} &= -\frac{2}{(v_4^2 - m_3^2)(k_1 + k_2)^2} \frac{m_4}{\sqrt{p_3^+ p_4^+}} \\
 &\quad \times \left[v_4^{\dot{A}B} (V_{\text{eff}})_{B\dot{B}} p_3^{\dot{B}0} + m_3^2 (V_{\text{eff}})^{\dot{A}0} \right] \iota^A, \\
 L_{8,+-}^{\dot{A}A} &= \frac{2}{(v_4^2 - m_3^2)(k_1 + k_2)^2} \frac{m_3 p_4^{\dot{A}0} \varepsilon_{\dot{B}\dot{C}}}{\sqrt{p_3^+ p_4^+}} \\
 &\quad \times \left[v_4^{\dot{B}A} (V_{\text{eff}})^{\dot{C}0} + (V_{\text{eff}})^{\dot{B}A} p_3^{\dot{C}0} \right]. \tag{3.42}
 \end{aligned}$$

3.4. Calculations

In order to illustrate our calculation methods, we will now compute the amplitude $R_{1,++}^\mu$ for both the massless and massive case.

In order to do that, we can use the fact that $P_1 = \sqrt{S}l_+$, $P_2 = \sqrt{S}l_-$, the eigenequations (2.18) and the completeness relation (2.40)

$$\begin{aligned}
 \frac{v_1^2 v_2^2}{2S} R_{1,++}^\mu &= \frac{1}{2} \langle p_3 | P_+ \gamma^\mu \hat{v}_1 \hat{l}_+ \hat{v}_2 \hat{l}_- | -p_4 \rangle \\
 &= \frac{1}{2} \langle p_3 | \gamma^\mu \hat{v}_1 (|\uparrow\rangle \langle\uparrow| + |\uparrow\rangle \langle\uparrow|) \hat{v}_2 (|\downarrow\rangle \langle\downarrow| + |\downarrow\rangle \langle\downarrow|) | -p_4 \rangle \\
 &= \frac{1}{2} \langle p_3 | \gamma^\mu \hat{v}_1 |\uparrow\rangle \langle\uparrow| \hat{v}_2 |\downarrow\rangle \langle\downarrow| | -p_4 \rangle. \tag{3.43}
 \end{aligned}$$

With the help of (2.40) and (2.43), we evaluate

$$\langle\uparrow| \hat{v}_2 |\downarrow\rangle = -v_2^\perp, \quad \langle\downarrow| -p_4\rangle = -\sqrt{p_4^+}. \tag{3.44}$$

Next we will insert the identity between γ^μ and \widehat{v}_1 using the completeness relation (2.41) to obtain

$$(3.43) = \frac{v_2^\perp \sqrt{p_4^+}}{2} (\langle p_3 | \gamma^\mu | \uparrow \rangle [\downarrow | \widehat{v}_1 | \uparrow] - \langle p_3 | \gamma^\mu | \downarrow \rangle [\uparrow | \widehat{v}_1 | \uparrow]) . \quad (3.45)$$

Then again from (2.40), we get $[\downarrow | \widehat{v}_1 | \uparrow] = -v_1^\perp$, $[\uparrow | \widehat{v}_1 | \uparrow] = v_1^-$, and also we decompose $\langle p_3 |$ with (2.43). These procedures lead to

$$\begin{aligned} (3.45) &= -\frac{v_2^\perp}{2} \sqrt{\frac{p_4^+}{p_3^+}} \left[v_1^\perp \left(p_3^+ \langle \uparrow | \gamma^\mu | \uparrow \rangle + p_3^\perp \langle \downarrow | \gamma^\mu | \uparrow \rangle \right) \right. \\ &\quad \left. + v_1^- \left(p_3^+ \langle \uparrow | \gamma^\mu | \downarrow \rangle + p_3^\perp \langle \downarrow | \gamma^\mu | \downarrow \rangle \right) \right] \\ &= -v_2^\perp \sqrt{\frac{p_4^+}{p_3^+}} (v_1^\perp p_3^+ \quad v_1^- p_3^\perp \quad v_1^\perp p_3^\perp \quad v_1^- p_3^+)^\mu . \end{aligned} \quad (3.46)$$

We can also calculate the amplitude using the abstract index notation in the spinor form

$$\begin{aligned} \frac{v_1^2 v_2^2 \sqrt{p_3^+ p_4^+}}{2S} R_{1,++}^{\dot{A}\dot{A}} &= \frac{\sqrt{p_3^+ p_4^+}}{2S} \langle p_3 | P_+ \gamma^{\dot{A}\dot{A}} \widehat{v}_1 \widehat{P}_1 \widehat{v}_2 \widehat{P}_2 | -p_4 \rangle \\ &= [0 \quad (p_3)_{1\dot{B}}] \begin{bmatrix} 0 & 0 \\ \varepsilon^{\dot{A}\dot{B}} \varepsilon^{AB} & 0 \end{bmatrix} \begin{bmatrix} 0 & (v_1)_{\dot{B}\dot{C}} \\ v_1^{\dot{B}C} & 0 \end{bmatrix} \begin{bmatrix} 0 & o_C \bar{o}_{\dot{C}} \\ o^C \bar{o}^{\dot{C}} & 0 \end{bmatrix} \\ &\times \begin{bmatrix} 0 & (v_2)_{C\dot{D}} \\ v_2^{\dot{C}D} & 0 \end{bmatrix} \begin{bmatrix} 0 & \iota_D \bar{\iota}_{\dot{D}} \\ \iota^D \bar{\iota}^{\dot{D}} & 0 \end{bmatrix} \begin{bmatrix} -(p_4)_{D\dot{I}} \\ 0 \end{bmatrix} \\ &= -(p_3)_{1\dot{B}} \varepsilon^{\dot{A}\dot{B}} \varepsilon^{AB} (v_1)_{\dot{B}\dot{C}} \bar{o}^{\dot{C}} o^C (v_2)_{C\dot{D}} \iota^D \bar{\iota}^{\dot{D}} (p_4)_{D\dot{I}} \\ &= -(p_3)_1^{\dot{A}} (v_1)_{\dot{0}}^A (v_2)_{0\dot{I}} (p_4)_{1\dot{I}} = -p_4^{\dot{0}\dot{0}} v_2^{\dot{0}\dot{1}} p_3^{\dot{A}\dot{0}} v_1^{\dot{1}A} . \end{aligned} \quad (3.47)$$

For the massive case it is a little bit more complicated. If we want to get the result in bracket notation in vector form, we should multiply all the terms and then use the completeness relation in each term.

In the spinor abstract index notation, the complication of the massive cases comes from the fact that now not all the matrices are antidiagonal and the bispinors contain more terms. Let us again consider the first amplitude as an example

$$\begin{aligned}
& \frac{\sqrt{p_3^+ p_4^+}}{2S} \langle p_3 | P_+ \gamma^{AA} (\hat{v}_1 + m_4) \hat{P}_1 (\hat{v}_2 + m_4) \hat{P}_2 | -p_4 \rangle \\
&= [m_3 \iota^B \quad (p_3)_{1\dot{B}}] \begin{bmatrix} 0 & 0 \\ \varepsilon^{\dot{A}\dot{B}} \varepsilon^{AB} & 0 \end{bmatrix} \begin{bmatrix} m_4 \delta_B^C & (v_1)_{B\dot{C}} \\ v_1^{\dot{B}C} & m_4 \delta_{\dot{C}}^B \end{bmatrix} \begin{bmatrix} 0 & o_C \bar{o}_{\dot{C}} \\ o^C \bar{o}^{\dot{C}} & 0 \end{bmatrix} \\
&\times \begin{bmatrix} m_4 \delta_C^D & (v_2)_{C\dot{D}} \\ v_2^{\dot{C}D} & m_4 \delta_{\dot{D}}^C \end{bmatrix} \begin{bmatrix} 0 & \iota_D \bar{\iota}_{\dot{D}} \\ \iota^D \bar{\iota}^{\dot{D}} & 0 \end{bmatrix} \begin{bmatrix} -(p_4)_{D\dot{I}} \\ m_4 \bar{\iota}^D \end{bmatrix} \\
&= -p_4^{\dot{0}0} p_3^{A0} \left[v_2^{\dot{0}1} v_1^{\dot{1}A} + m_4^2 o^A \right]. \tag{3.48}
\end{aligned}$$

To obtain the final result, one has to perform the matrix multiplication and then contract and raise some spinor indices.

3.5. Comparison with the trace method

For the purpose of this subsection only, we denote the spinorial matrix appearing in the amplitude A_n^μ by \mathfrak{A}_n^μ

$$A_n^\mu = \bar{u}_{\sigma_3}(p_3) \mathfrak{A}_n^\mu v_{\sigma_4}(p_4). \tag{3.49}$$

In an analogous way, we define the matrices $\mathfrak{A}_S^\mu, \mathfrak{A}_A^\mu$.

The amplitudes squared (3.15) summed also over spins of $q\bar{q}$ can be computed as traces. For the symmetric part

$$\sum_{\sigma_3, \sigma_4} \mathcal{M}_S^{\mu\nu} = \frac{g^4 (N^2 - 2)}{2N (N^2 - 1)} \text{Tr} \left[(\hat{p}_3 + m_3) \mathfrak{A}_S^\mu (\hat{p}_4 - m_4) \mathfrak{A}_S^{\dagger\nu} \right], \tag{3.50}$$

and for the antisymmetric

$$\sum_{\sigma_3, \sigma_4} \mathcal{M}_A^{\mu\nu} = \frac{g^4 N}{2 (N^2 - 1)} \text{Tr} \left[(\hat{p}_3 + m_3) \mathfrak{A}_A^\mu (\hat{p}_4 - m_4) \mathfrak{A}_A^{\dagger\nu} \right]. \tag{3.51}$$

Using the trace formulas (3.50) and (3.51), we checked numerically the helicity structure functions of the form

$$\epsilon_\mu^{(r)*} \mathcal{M}_S^{\mu\nu} \epsilon_\nu^{(r')}, \quad \epsilon_\mu^{(r)*} \mathcal{M}_A^{\mu\nu} \epsilon_\nu^{(r')}, \tag{3.52}$$

where $r, r' \in \{+, -, 0\}$ are basis polarizations of V^* defined in a chosen reference frame. Up to negligible numerical errors, they agree with results obtained by directly evaluating amplitudes using our analytic formulas. The numerical checks were performed using the Wolfram **Mathematica** [25]. The used code is available upon request.

4. Outlook

We presented compact analytic forms of the $g^*g^* \rightarrow \bar{q}qV^*$ scattering amplitudes. Evaluation of these scattering amplitudes is needed as a subroutine in programs evaluating numerically the Drell–Yan structure functions, and it is inefficient if performed using trace methods [15]. Our result can be used to speed up numerical calculations in such studies, and it could be used in event generators [26]. The calculation method we have used can be applied to other processes treated in the k_T -factorization framework at the leading order. Spinor helicity methods can also be applied in NLO calculations, *e.g.* to obtain the real radiative corrections. One loop amplitudes involving an off-shell gluon have been considered in [27], which also uses the spinor helicity formalism.

We would like to thank Leszek Motyka for introducing us to the topic of the Drell–Yan process, discussions, and reading of the manuscript. This research was supported by the National Science Centre (NCN), Poland, grant No. 2017/27/B/ST2/02755.

REFERENCES

- [1] S.D. Drell, T.M. Yan, «Massive Lepton Pair Production in Hadron–Hadron Collisions at High-Energies», *Phys. Rev. Lett.* **25**, 316 (1970); *Erratum ibid.* **25**, 902 (1970).
- [2] J.C. Collins, R.K. Ellis, «Heavy quark production in very high-energy hadron collisions», *Nucl. Phys. B* **360**, 3 (1991).
- [3] S. Catani, F. Hautmann, «High-energy factorization and small- x deep inelastic scattering beyond leading order», *Nucl. Phys. B* **427**, 475 (1994), [arXiv:hep-ph/9405388](#).
- [4] S. Catani, M. Ciafaloni, F. Hautmann, «High-energy factorization and small- x heavy flavor production», *Nucl. Phys. B* **366**, 135 (1991).
- [5] S. Catani, M. Ciafaloni, F. Hautmann, «Gluon contributions to small x heavy flavor production», *Phys. Lett. B* **242**, 97 (1990).
- [6] R. Angeles-Martinez *et al.*, «Transverse Momentum Dependent (TMD) Parton Distribution Functions: Status and Prospects», *Acta Phys. Pol. B* **46**, 2501 (2015), [arXiv:1507.05267 \[hep-ph\]](#).
- [7] ATLAS Collaboration (G. Aad *et al.*), «Measurement of the angular coefficients in Z -boson events using electron and muon pairs from data taken at $\sqrt{s} = 8$ TeV with the ATLAS detector», *J. High Energy Phys.* **2016**, 159 (2016), [arXiv:1606.00689 \[hep-ex\]](#).
- [8] A. Gehrmann-De Ridder *et al.*, «Precise QCD Predictions for the Production of a Z Boson in Association with a Hadronic Jet», *Phys. Rev. Lett.* **117**, 022001 (2016), [arXiv:1507.02850 \[hep-ph\]](#).

- [9] A. Gehrmann-De Ridder *et al.*, «The NNLO QCD corrections to Z boson production at large transverse momentum», *J. High Energy Phys.* **2016**, 133 (2016), [arXiv:1605.04295 \[hep-ph\]](#).
- [10] R. Gauld *et al.*, «Precise predictions for the angular coefficients in Z -boson production at the LHC», *J. High Energy Phys.* **2017**, 003 (2017), [arXiv:1708.00008 \[hep-ph\]](#).
- [11] X. Li, B. Yan, C.P. Yuan, «Lam–Tung relation breaking in Z boson production as a probe of SMEFT effects», [arXiv:2405.04069 \[hep-ph\]](#).
- [12] S. Piloneta, A. Vladimirov, «Angular distributions of Drell–Yan leptons in the TMD factorization approach», [arXiv:2407.06277 \[hep-ph\]](#).
- [13] C.S. Lam, W.K. Tung, «Parton-model relation without quantum-chromodynamic modifications in lepton pair production», *Phys. Rev. D* **21**, 2712 (1980).
- [14] J.C. Peng, W.C. Chang, R.E. McClellan, O. Teryaev, «Interpretation of Angular Distributions of Z -boson Production at Colliders», *Phys. Lett. B* **758**, 384 (2016), [arXiv:1511.08932 \[hep-ph\]](#).
- [15] L. Motyka, M. Sadzikowski, T. Stebel, «Lam–Tung relation breaking in Z^0 hadroproduction as a probe of parton transverse momentum», *Phys. Rev. D* **95**, 114025 (2017), [arXiv:1609.04300 \[hep-ph\]](#).
- [16] M. Deak, F. Schwennsen, « Z and W^\pm production associated with quark–antiquark pair in k_T -factorization at the LHC», *J. High Energy Phys.* **2008**, 035 (2008), [arXiv:0805.3763 \[hep-ph\]](#).
- [17] S. Benić, K. Fukushima, O. Garcia-Montero, R. Venugopalan, «Probing gluon saturation with next-to-leading order photon production at central rapidities in proton–nucleus collisions», *J. High Energy Phys.* **2017**, 115 (2017), [arXiv:1609.09424 \[hep-ph\]](#).
- [18] S. Benić, K. Fukushima, O. Garcia-Montero, R. Venugopalan, «Constraining unintegrated gluon distributions from inclusive photon production in proton–proton collisions at the LHC», *Phys. Lett. B* **791**, 11 (2019), [arXiv:1807.03806 \[hep-ph\]](#).
- [19] R. Kleiss, W.J. Stirling, «Spinor techniques for calculating $pp \rightarrow W^\pm/Z^0 + \text{jets}$ », *Nucl. Phys. B* **262**, 235 (1985).
- [20] N. Arkani-Hamed, T.C. Huang, Y.t. Huang, «Scattering amplitudes for all masses and spins», *J. High Energy Phys.* **2021**, 070 (2021), [arXiv:1709.04891 \[hep-th\]](#).
- [21] R. Penrose, W. Rindler, «Spinors and Space-Time, Volume 1: Two-Spinor Calculus and Relativistic Fields 1», *Cambridge University Press*, 1984.
- [22] A. van Hameren, P. Kotko, K. Kutak, «Helicity amplitudes for high-energy scattering», *J. High Energy Phys.* **2013**, 078 (2013), [arXiv:1211.0961 \[hep-ph\]](#).
- [23] S.P. Baranov, A.V. Lipatov, N.P. Zotov, «Production of electroweak gauge bosons in off-shell gluon–gluon fusion», *Phys. Rev. D* **78**, 014025 (2008), [arXiv:0805.4821 \[hep-ph\]](#).

- [24] L.N. Lipatov, «Gauge invariant effective action for high-energy processes in QCD», *Nucl. Phys. B* **452**, 369 (1995), [arXiv:hep-ph/9502308](#).
- [25] Wolfram Research, Inc., Mathematica, Version 13.3, Champaign, IL, 2024.
- [26] A. van Hameren, «KaTie: For parton-level event generation with k_T -dependent initial states», *Comput. Phys. Commun.* **224**, 371 (2018), [arXiv:1611.00680 \[hep-ph\]](#).
- [27] E. Blanco, A. Giachino, A. van Hameren, P. Kotko, «One-loop gauge invariant amplitudes with a space-like gluon», *Nucl. Phys. B* **995**, 116322 (2023), [arXiv:2212.03572 \[hep-ph\]](#).